SLAC-PUB- 5730
March, 1992
T/E

Estimation of Oblique Electroweak Corrections

TATSU TAKEUCHI*

Stanford Linear Accelerator Center
Stanford University, Stanford, California 94309

ABSTRACT

I will first review the experimental limits placed on the oblique correction parameters S and T. Then, I will discuss how the value of S can be estimated for running and walking technicolor theories.

A talk presented at
The International Workshop on Electroweak Symmetry Breaking.
Hiroshima, Japan, November 12–15, 1991.

* Work supported by the Department of Energy, contract DE–AC03–76SF00515.

1. Introduction

In the past few years, the accuracy in which various electroweak observables have been measured have reached the level which enables us to put limits on the sizes of the oblique electroweak correction parameters S, T, and U. These three parameters are measures of the size of radiative corrections coming from new physics beyond the Standard Model. Therefore, putting experimental limits on them provides us with valuable information on the yet inaccessible high energy sectors.

On the other hand, whether we will be able to make use of this information effectively or not rests on our ability to calculate these parameters reliably from theory. For technicolor and other strongly interacting theories, this is a difficult task since perturbation theory cannot be used. In this talk, I would like to focus on how one may estimate the size of the parameter S for technicolor theories by making use of dispersion relations.

This talk is organized as follows. In section 2, I review the definitions of S, T, and U, emphasizing the assumptions that are necessary to describe the corrections from new physics with just these three parameters. In section 3, I review the current experimental limits on S and T, and discuss the dependence of these limits on the choice of m_t and m_H in the reference Standard Model. In section 4, I discuss how the value of S may be estimated for running technicolor theories by expressing S in terms of a dispersion integral. In sections 5, I discuss how the estimates given in section 4 may be modified for walking technicolor theories. In section 6, I compare the estimates of S with the experimental limits and state some conclusions.

2. The S, T, U Parameters

The validity of expressing the effect of radiative corrections coming from new physics beyond the Standard Model with just three parameters S, T, and U, hinges on three basic assumptions. They are:

[1] The gauge group of the electroweak interactions is $SU(2)_L \times U(1)_Y$. There are no electroweak gauge bosons other than the photon, the W's, and the Z.

[2] The couplings of new physics to light fermions are suppressed compared to their couplings to the electroweak gauge bosons.

[3] The intrinsic scale of the new physics is large compared to the masses of the W's and the Z.

All precision electroweak measurements probe processes that are described at tree level by an electroweak gauge boson exchange between light fermions. Corrections to these processes come in three classes: vacuum polarization, vertex,

and box corrections. The second assumption implies that the contribution of new physics to vertex and box corrections are suppressed compared to their contribution to vacuum polarization corrections. Therefore, as long as we restrict our attention to corrections from new physics, we can neglect vertices and boxes and concentrate on the vacuum polarizations, *i.e.* the so called 'oblique' corrections.

The first assumption tells us that there are four vacuum polarizations that must be taken into account. Namely, the gauge boson self–energies $\Pi_{AA}(q^2)$, $\Pi_{ZZ}(q^2)$, $\Pi_{WW}(q^2)$, and the Z–photon mixing $\Pi_{ZA}(q^2)$. Let me introduce some notation. Let J^μ_Q, J^μ_3, and $J^\mu_\pm = J^\mu_1 \pm iJ^\mu_2$ denote the currents coupling to the electroweak gauge bosons via

$$\frac{e}{\sqrt{2}s}\left(W^+_\mu J^\mu_+ + W^-_\mu J^\mu_-\right) + \frac{e}{sc}Z_\mu\left(J^\mu_3 - s^2 J^\mu_Q\right) + eA_\mu J^\mu_Q, \tag{2.1}$$

where $s = \sin\theta_w$ and $c = \cos\theta_w$. I define the vacuum polarization amplitudes Π_{XY}, where $(XY) = (11), (22), (33), (QQ), (3Q)$, by

$$ig^{\mu\nu}\Pi_{XY}(q^2) + (q^\mu q^\nu \text{ terms}) \equiv \int d^4x e^{-iqx}\left\langle J^\mu_X(x) J^\nu_Y(0)\right\rangle, \tag{2.2}$$

and Π'_{XY} by

$$\Pi_{XY}(q^2) = \Pi_{XY}(0) + q^2\Pi'_{XY}(q^2). \tag{2.3}$$

The unbroken $U(1)$ symmetry of electromagnetism implies $\Pi_{11}(q^2) = \Pi_{22}(q^2)$, and $\Pi_{3Q}(0) = \Pi_{QQ}(0) = 0$. Then, the self energies of the electroweak gauge bosons and the Z–photon mixing can be written down as follows:

$$\begin{aligned}
\Pi_{AA} &= e^2\Pi_{QQ}, \\
\Pi_{ZA} &= \frac{e^2}{sc}\left(\Pi_{3Q} - s^2\Pi_{QQ}\right), \\
\Pi_{ZZ} &= \frac{e^2}{s^2c^2}\left(\Pi_{33} - 2s^2\Pi_{3Q} + s^4\Pi_{QQ}\right), \\
\Pi_{WW} &= \frac{e^2}{s^2}\Pi_{11}.
\end{aligned} \tag{2.4}$$

These relations show that we can either discuss oblique corrections in terms of the four functions Π_{AA}, Π_{ZA}, Π_{ZZ}, and Π_{WW}, or equivalently, in terms of the four functions Π_{QQ}, Π_{3Q}, Π_{33}, and Π_{11}.

Let us divide the Π_{XY}'s into two parts: The contribution of the Standard Model Π^{sm}_{XY}, and the contribution of new physics beyond the Standard Model Π^{new}_{XY}.

$$\Pi_{XY}(q^2) = \Pi^{sm}_{XY}(q^2) + \Pi^{new}_{XY}(q^2). \tag{2.5}$$

The contribution of the three generations of quarks and leptons, the gauge bosons, and the Standard Model Higgs sector are included in Π^{sm}_{XY}. A slight complication arises here when considering the possibility that the true Higgs sector is not that of the Standard Model. In that case, the contribution of the true Higgs sector is included in Π^{new}_{XY}, but at the same time the contribution of the Standard Model Higgs sector must be subtracted out of Π^{new}_{XY} so that it cancels in the sum $\Pi_{XY} = \Pi^{sm}_{XY} + \Pi^{new}_{XY}$. This makes Π^{new}_{XY} depend on the value of m_H chosen for the reference Standard Model in calculating Π^{sm}_{XY}. (At the one loop level, however, there is no m_H dependence in Π^{sm}_{QQ} or Π^{sm}_{3Q} because the Standard Model Higgs boson is chargeless and does not couple directly to the photon. Therefore, there is no m_H dependence in Π^{new}_{QQ} or Π^{new}_{3Q} either.)

The third assumption lets us expand the Π^{new}_{XY}'s around $q^2 = 0$ and neglect terms of order q^4 and above while making only a relative error of (m_Z^2/m^2_{new}), where m_{new} is the intrinsic scale of the new physics:

$$\begin{aligned}
\Pi^{new}_{QQ}(q^2) &\approx q^2 \Pi'^{new}_{QQ}(0), \\
\Pi^{new}_{3Q}(q^2) &\approx q^2 \Pi'^{new}_{3Q}(0), \\
\Pi^{new}_{33}(q^2) &\approx \Pi^{new}_{33}(0) + q^2 \Pi'^{new}_{33}(0), \\
\Pi^{new}_{11}(q^2) &\approx \Pi^{new}_{11}(0) + q^2 \Pi'^{new}_{11}(0).
\end{aligned} \tag{2.6}$$

Please note that when Π^{new}_{XY} includes the (negative) contribution of the Standard Model Higgs sector, we must take the Higgs boson mass m_H in the reference Standard Model to be large compared to m_Z for this approximation to be valid. This will inevitably take m_H out of the region permitted by triviality arguments[1] but there is no need for concern since the Higgs boson contribution will cancel out in the end. Of course, if we are assuming that the true Higgs sector is that of the Standard Model, there is no need for these considerations.

The above expansion lets us reduce the number of parameters that describe the corrections from new physics to six: $\Pi'^{new}_{QQ}(0)$, $\Pi'^{new}_{3Q}(0)$, $\Pi^{new}_{33}(0)$, $\Pi'^{new}_{33}(0)$, $\Pi^{new}_{11}(0)$, and $\Pi'^{new}_{11}(0)$. Three linear combinations of these parameters are absorbed into renormalizations of g, g', and v. This leaves us with only three

observable parameters which can be taken be

$$\begin{aligned}
\alpha S &\equiv 4e^2 \left[\Pi'^{new}_{33}(0) - \Pi'^{new}_{3Q}(0)\right], \\
\alpha T &\equiv \frac{e^2}{s^2 c^2 m_Z^2} \left[\Pi^{new}_{11}(0) - \Pi^{new}_{33}(0)\right], \\
\alpha U &\equiv 4e^2 \left[\Pi'^{new}_{11}(0) - \Pi'^{new}_{33}(0)\right].
\end{aligned} \tag{2.7}$$

The ultraviolet divergences cancel exactly between the Π's on the right hand sides of these definitions so that S, T, and U are finite and well defined without any regularization.

Using S, T, and U, the value of a general observable x after radiative corrections can be written as

$$x = x_{sm}(m_t, m_H) + a_x S + b_x T + c_x U, \tag{2.8}$$

where $x_{sm}(m_t, m_H)$ is the prediction of the Standard Model including radiative corrections from the Standard Model itself. If the true Higgs sector is not that of the Standard Model, the m_H dependence of the Π^{new}_{XY}'s will make S, T, U depend on m_H, and the m_H dependence will cancel between $x_{sm}(m_t, m_H)$ and S, T, U to make the prediction x independent of m_H. The coefficients a_x, b_x, and c_x are independent of m_t or m_H, and can be derived for each observable x using the star–function formalism of Kennedy and Lynn[2,3,4].

It should be noted, however, that both $x_{sm}(m_t, m_H)$ and the coefficients a_x, b_x, c_x depend on the so called 'renormalization scheme'; namely, which three observables are used as input to fix g, g', and v. A particularly convenient choice is to use α, G_F, and m_Z as input. In this case, it can be shown that $c_x = 0$ for all the neutral current and low energy observables.[3,4] This means that the number of parameters that describe radiative corrections from new physics can be further reduced to two for the neutral current and low energy observables which comprise the bulk of precision electroweak measurement data. In the appendix, I list the expressions corresponding to Eq. (2.8) for the observables listed in table 1 for this choice of input parameters, and the reference values $m_t = 150\text{GeV}$ and $m_H = 1\text{TeV}$.

Table 1. The precision measurements used in the S–T maximum likelihood analysis.

Observable	Measured Value	Reference	Standard Model
g_L^2	0.2977 ± 0.0042	5	0.3001
g_R^2	0.0317 ± 0.0034	5	0.0302
m_W/m_Z	0.8790 ± 0.0030	6	0.8787
Γ_Z [GeV]	2.487 ± 0.010	7	2.484
$R_Z = \Gamma_{\rm had}/\Gamma_{\ell^+\ell^-}$	20.89 ± 0.13	7	20.78
A_{FB}^{ℓ}	0.0138 ± 0.0049	7	0.0126
A_{FB}^{b}	0.126 ± 0.022	8	0.0848
P_τ	-0.134 ± 0.035	8	-0.1297
$Q_W(^{133}_{55}\mathrm{Cs})$	-71.04 ± 1.81	9	-73.31

3. The Experimental Limits on S and T

Since the neutral current and low energy observables depend only on S and T (for the right choice of renormalization scheme), by comparing their measured values with the expressions given in the appendix, we can put constraints on the possible values of S and T permitted by experiment. Furthermore, we can expect U to be small compared to T in general, since our approximation Eq. (2.6) implies

$$U = 16\pi \left[\Pi'^{new}_{11}(0) - \Pi'^{new}_{33}(0)\right] \sim 16\pi \left[\frac{\Pi^{new}_{11}(0) - \Pi^{new}_{33}(0)}{m^2_{new}}\right] \sim \left(\frac{m_Z^2}{m^2_{new}}\right) T. \tag{3.1}$$

Therefore, we can make the additional assumption that $U \approx 0$, and use the only accurately measured charged current observable, namely m_W, to restrict S and T also.

A precise measurement of an observable x will restrict S and T onto the line

$$x_{exp} = x_{sm}(m_t, m_H) + a_x S + b_x T, \tag{3.2}$$

where x_{exp} is the measured value of x. In practice, all measurements have associated errors so the line will become blurred into a band on the S–T plane. In figures 1 and 2, I show the bands corresponding to the measurements listed in table 1, where the widths of the bands correspond to 1σ errors. The origin of the S–T plane corresponds to the reference Standard Model with $m_t = 150$GeV

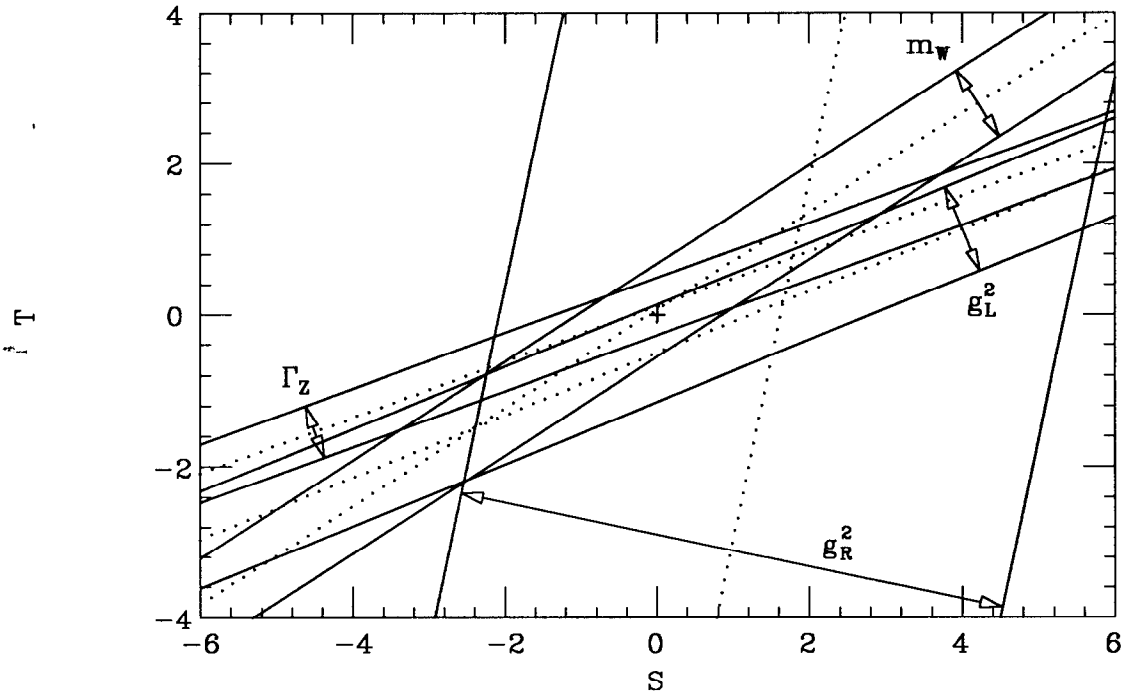

Figure 1. 1σ bands in the S–T plane for the first four measurements listed in Table 1.

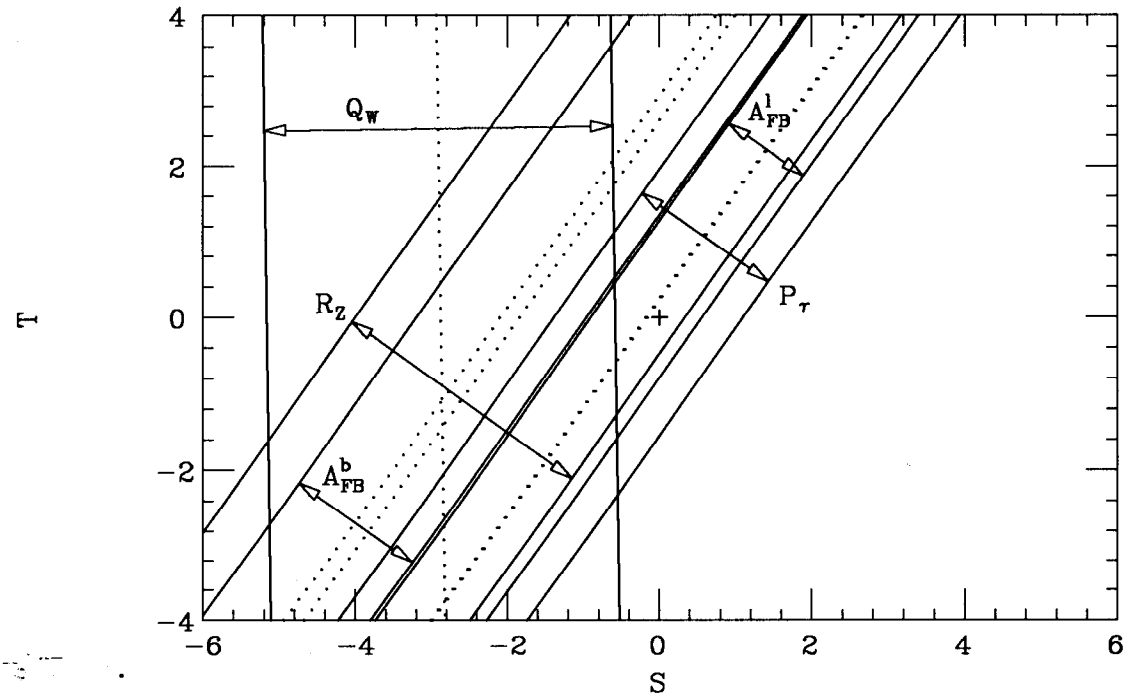

Figure 2. 1σ bands in the S–T plane for the last five measurements listed in Table 1.

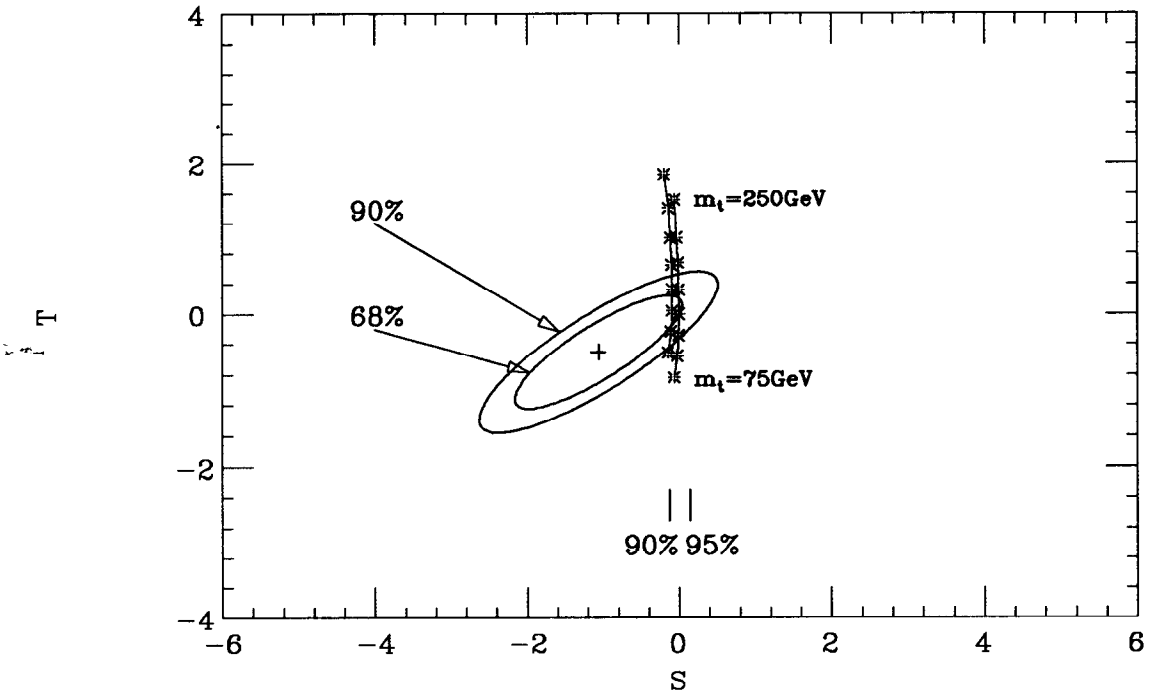

Figure 3. Coutours of the likelihood function of S and T corresponding to 68% and 90% probabilities, computed from the measurements listed in Table 1. The notches at the bottom of the figure correspond to the 90% and 95% confidence upper limits on S.

and $m_H = 1\text{TeV}$. Just by inspection, we can see that the overlap of the bands is greatest in the third quadrant of the S–T plane. A maximum likelihood analysis yields

$$\begin{aligned} S &= -1.06 \pm 0.73, \\ T &= -0.50 \pm 0.49, \\ \text{cov}(S,T) &= 0.30, \end{aligned} \tag{3.3}$$

where $\text{cov}(S,T)$ is the covariance between S and T. Figure 3 shows the point of maximum likelihood with the 68% and 90% confidence level contours around it.

As is evident from Eq. (3.2), the experimental limits on S and T differ depending on the values of m_t and m_H chosen for the reference Standard Model. Actually, for a given set of observables, it can be shown that only the central values of S and T depend on m_t and m_H, and that their errors and covariance do not. Graphically, this means that the shapes and sizes of the likelihood contours will stay the same, and only their positions on the S–T plane will shift with m_t and m_H.

Table 2. The values of m_t and m_H used for the reference Standard Model in various references. (In ref. 13, no Standard Model subtraction is made.)

Reference	m_t	m_H
10	150 GeV	1 TeV
11	140 GeV	100 GeV
12	m_Z	m_Z
13	—	—
14	150 GeV	100 GeV
15	140 GeV	100 GeV
16	140 GeV	300 GeV

Instead of displaying the position of the likelihood contours relative to the origin of the S–T plane for different values of m_t and m_H, I choose to keep the likelihood contours fixed and plot the position of origin of the S–T plane relative to the likelihood contours. The asterisks in figure 3 show where the origin would be relative to the likelihood contours for the choices $m_H = 1\text{TeV}$ and $m_H = 100\text{GeV}$ for the Higgs boson mass, and $m_t = 75\text{GeV}$ up to $m_t = 250\text{GeV}$ at 25GeV intervals for the t-quark mass. The asterisks corresponding to the same choice of m_H are connected with lines, with the $m_H = 1\text{TeV}$ case on the right and the $m_H = 100\text{GeV}$ case on the left. The $m_t = 75\text{GeV}$ case is at the bottom of these lines, and the $m_t = 250\text{GeV}$ case is at the top.

Many authors have analysed precision electroweak measurements to put limits on S and T. Since the choice of the reference values for m_t and m_H differ from author to author, care must be taken when quoting or comparing results. Table 2 lists the values of m_t and m_H used in various references. For some reason, a popular choice for the reference value of m_H seems to be 100GeV. However, as I stated in the previous section, if we are considering modifications to the Higgs sector, such as technicolor, the value of m_H for the reference Standard Model should be taken to be large compared to m_Z to justify our approximation in Eq. (2.6).

4. Estimation of S for Technicolor

4.1 The Assumptions

Let us now turn to the main topic of this talk. Namely, the estimation of the oblique correction parameters for technicolor.

In the following, I will assume for simplicity that isospin and parity are conserved in the technisector. This assumption prevents us from introducing extended technicolor (ETC) interactions that give different masses to quarks and leptons belonging to the same $SU(2)_L$ doublet since such interactions necessarily break both isospin and parity. I will also assume that the technicolor dynamics is QCD–like, *i.e.* that we can infer much about technicolor by looking at QCD. Such QCD–like technicolor theories are known to be plagued by excessive flavor changing neutral currents (FCNC's) from ETC interactions. Therefore, it should be noted that the technicolor theories I will consider here are unrealistic. However, they do provide a good starting point in our attempt to estimate S and T for strongly interacting theories.

The conservation of isospin in the technisector automatically means $T = 0$, so we can concentrate on estimating S. The strategy that I will pursue to estimate S is as follows. First, I represent S as a dispersion integral over the difference between the vector and axial–vector isospin–one spectral functions. Then, I model the spectral functions using three different methods: vector meson dominance, leading log approximation in chiral perturbation theory, and the rescaling of QCD data. The value of S will be calculated for each case and the reliability of the estimate discussed.

4.2 Dispersive Representation of S

I start by writing the electromagnetic and the left–handed isospin currents in terms of the conventional hypercharge current and the isospin vector and axial–vector currents:

$$\begin{aligned} J_3^\mu &= \frac{1}{2}\left[J_V^\mu - J_A^\mu\right], \\ J_Q^\mu &= J_V^\mu + \frac{1}{2}J_{B-L}^\mu. \end{aligned} \tag{4.1}$$

Note that J_V^μ and J_A^μ belong to isospin triplets while J_{B-L}^μ is an isospin singlet. Since we assume isospin and parity conservation in the technisector, vacuum polarizations between currents of opposite parity or of different isospin vanish.

Therefore, the technisector contribution to Π_{33} and Π_{3Q} can be written as

$$\begin{aligned}\Pi^{tc}_{33} &= \frac{1}{4}\left[\Pi^{tc}_{VV} + \Pi^{tc}_{AA}\right], \\ \Pi^{tc}_{3Q} &= \frac{1}{2}\Pi^{tc}_{VV},\end{aligned} \tag{4.2}$$

where the Π's on the right hand side are defined as in Eq. (2.2). Note that since the technicolor interaction is assumed to spontaneously break the axial isospin symmetry, we have

$$\begin{aligned}\Pi^{tc}_{VV}(q^2) &= q^2\Pi'^{tc}_{VV}(q^2), \\ \Pi^{tc}_{AA}(q^2) &= \Pi^{tc}_{AA}(0) + q^2\Pi'^{tc}_{AA}(q^2) = F_\pi^2 + q^2\Pi'^{tc}_{AA}(q^2),\end{aligned} \tag{4.3}$$

where $F_\pi = 250\text{GeV}$ is the technipion decay constant. In terms of Π^{tc}_{VV} and Π^{tc}_{AA}, we find

$$S = -4\pi\left[\Pi'^{tc}_{VV}(0) - \Pi'^{tc}_{AA}(0)\right] - (\text{SM Higgs sector}). \tag{4.4}$$

The contribution of the Standard Model Higgs sector, which the technisector replaces, must be subtracted out as I commented earlier.

I define the spectral functions $R^{tc}_V(s)$ and $R^{tc}_A(s)$ by

$$\begin{aligned}R^{tc}_V(s) &\equiv -12\pi\text{Im}\Pi'^{tc}_{VV}(s), \\ R^{tc}_A(s) &\equiv -12\pi\text{Im}\Pi'^{tc}_{AA}(s).\end{aligned} \tag{4.5}$$

These functions are analogs of

$$R(s) = -12\pi\text{Im}\Pi'^{qcd}_{QQ}(s) = \left[\frac{3s}{4\pi\alpha^2}\right]\sigma(e^+e^- \to \gamma \to \text{hadrons}), \tag{4.6}$$

with the electromagnetic quark current replaced by the vector and axial–vector isospin–one technifermion currents. R^{tc}_V and R^{tc}_A are related to Π'^{tc}_{VV} and Π'^{tc}_{AA} through the dispersion relation

$$\Pi'^{tc}_{VV}(q^2) - \Pi'^{tc}_{AA}(q^2) = -\frac{1}{12\pi^2}\int_0^\infty ds\ \frac{R^{tc}_V(s) - R^{tc}_A(s)}{s - q^2}. \tag{4.7}$$

Taking the $q^2 \to 0$ limit, we find

$$S = \frac{1}{3\pi}\int_0^\infty \frac{ds}{s}\left\{\left[R^{tc}_V(s) - R^{tc}_A(s)\right] - \frac{1}{4}\left[1 - \left(1 - \frac{m_H^2}{s}\right)^3\theta(s - m_H^2)\right]\right\}. \tag{4.8}$$

The terms in the second set of brackets are the Standard Model Higgs sector

contributions.

4.3 General Behavior of $R_V^{tc}(s)$ and $R_A^{tc}(s)$

In order to use Eq. (4.8) to calculate S, we must know the spectral functions $R_V^{tc}(s)$ and $R_A^{tc}(s)$. Though it is impossible to obtain these spectral functions for a general value of s, they can be calculated in the two limits $s \to \infty$ and $s \to 0$. In the ultraviolet limit $s \to \infty$, the asymptotic freedom of technicolor implies that the spectral functions will approach the free technifermion result, namely, they will both be given by the sum of the squares of the technifermion isospins. Conversely, in the infrared limit $s \to 0$, the spectral functions can be calculated from a chiral Lagrangian constructed from the technipion and the pseudo–Goldstone boson (PGB) degrees of freedom. In particular, below any of the PGB masses only the technipions will contribute, and we will find that $R_V^{tc}(s) \to 1/4$ and $R_A^{tc}(s) \to 0$ as $s \to 0$. Note that because of this two technipion contribution to $R_V^{tc}(s)$, the contribution of the technisector alone would make S infrared divergent. This is due to the masslessness of the technipions. By subtracting the Standard Model Higgs sector contribution from the technisector contribution, the contribution of the exact Goldstone bosons in both sectors will cancel and we are left with a finite result.

Further information on the behavior of $R_V^{tc}(s)$ and $R_A^{tc}(s)$ can be obtained as follows. From Eqs. (4.3) and (4.7), we find

$$\Pi_{VV}^{tc}(q^2) - \Pi_{AA}^{tc}(q^2) = -\frac{q^2}{12\pi^2} \int_0^\infty ds \, \frac{R_V^{tc}(s) - R_A^{tc}(s)}{s - q^2} - F_\pi^2. \tag{4.9}$$

It can be shown that for asymptotically free theories, the left hand side falls asymptotically as $1/q^4$ in the limit $q^2 \to \infty$.[17] This means that if we expand the right hand side in inverse powers of q^2, the constant term and the $1/q^2$ term must vanish:

$$\begin{aligned} \int_0^\infty ds \left[R_V^{tc}(s) - R_A^{tc}(s)\right] &= 12\pi^2 F_\pi^2, \\ \int_0^\infty ds \; s \left[R_V^{tc}(s) - R_A^{tc}(s)\right] &= 0. \end{aligned} \tag{4.10}$$

These relations are known as the first and second Weinberg sum rules.[18]

The functional form of $R_V^{tc}(s)$ and $R_A^{tc}(s)$ in between the ultraviolet and infrared limits must be modeled using the Weinberg sum rules and our knowledge of QCD to guide us. It should be noted that the integral expression for S given in Eq. (4.8) is dominated in the infrared due to the factor $1/s$ multiplying the spectral functions. Therefore, it would be sufficient for our model to capture the low momentum behavior of the spectral functions accurately.

4.4 Vector Meson Dominance

Let me first model $R_V^{tc}(s)$ and $R_A^{tc}(s)$ using vector meson dominance in which both spectral functions are saturated by the pole of the lowest lying resonances:

$$\begin{aligned} R_V^{tc}(s) &= 12\pi^2 F_\rho^2 \delta(s - M_\rho^2), \\ R_A^{tc}(s) &= 12\pi^2 F_{a_1}^2 \delta(s - M_{a_1}^2). \end{aligned} \tag{4.11}$$

Though this is an extremely crude approximation, it models a prominent feature of the spectral functions and is known to work fairly well for QCD. Imposing the Weinberg sum rules Eq. (4.10) on these expressions gives us

$$F_\rho^2 = \left(\frac{M_{a_1}^2}{M_{a_1}^2 - M_\rho^2}\right) F_\pi^2, \qquad F_{a_1}^2 = \left(\frac{M_\rho^2}{M_{a_1}^2 - M_\rho^2}\right) F_\pi^2. \tag{4.12}$$

Using this result, we find

$$S = \frac{1}{3\pi}\int_0^\infty \frac{ds}{s}\left[R_V^{tc}(s) - R_A^{tc}(s)\right] = 4\pi\left(1 + \frac{M_\rho^2}{M_{a_1}^2}\right)\frac{F_\pi^2}{M_\rho^2}. \tag{4.13}$$

I did not make the Standard Model subtraction here because Eq. (4.11) does not include the two technipion contribution to begin with. Rescaling this expression to QCD units, we find

$$S \approx 4\pi\left(1 + \frac{m_\rho^2}{m_{a_1}^2}\right)\frac{f_\pi^2}{m_\rho^2}\frac{N_{tc}}{3}\frac{N_{tf}}{2} \approx 0.25\frac{N_{tc}}{3}\frac{N_{tf}}{2} \tag{4.14}$$

where N_{tc} and N_{tf} are the numbers of technicolors and techniflavors, respectively. I use upper (lower) case letters for the technicolor (QCD) decay constants and masses. Note that of the 0.25, the techni–ρ contribution is 0.29 while the techni–a_1 contribution is only -0.04. In this model, the value of S is totally dominated by the contribution of the techni–ρ.

4.5 Leading Log Approximation in Chiral Perturbation Theory

The second model I will consider is chiral perturbation theory in which only the technipions and the pseudo–Goldstone boson (PGB) degrees of freedom are considered. At the one–loop level,

$$R_V^{tc} = \frac{1}{4}\left[1 + \sum_i \left(1 - \frac{4M_{P_i}^2}{s}\right)^{3/2} \theta(s - 4M_{P_i}^2)\right], \qquad (4.15)$$
$$R_A^{tc} = 0,$$

where the sum runs over the $[(N_{tf}/2)^2 - 1]$ pairs of PGB's. These expressions are only valid well below the lowest lying resonance, the techni–ρ, but since the integral for S is dominated in the infrared, integrating these expressions in their region of validity could give a rough estimate of S. Plugging Eq. (4.15) into Eq. (4.8) and cutting the integral off at the techni–ρ mass, we find

$$S \approx \frac{1}{12\pi} \sum_i \left(\log \frac{M_\rho^2}{M_{P_i}^2}\right). \qquad (4.16)$$

For a minimal technicolor model with $N_{tf} = 2$, this approximation gives $S \approx 0$ since there are no PGB's in the model. For a one–generation technicolor model with $N_{tf} = 8$, $M_\rho = 1\text{TeV}$, and a common mass $M_P = 200\text{GeV}$ for the 15 pairs of PGB's, we get $S \approx 1.3$.

4.6 Rescaling of QCD Data

Comparing the results of the vector meson dominance model and the chiral log approximation, we notice that the dependence of S on N_{tc} and N_{tf} are completely different for the two cases. In the vector meson dominance model S is proportional to $N_{tc}N_{tf}$, while in the chiral log approximation S is proportional to N_{tf}^2. This difference is due to the fact that the each model emphasizes a different feature of the spectral functions, the vector meson resonances in one case, and the PGB contributions in the other. Since both models give comparable estimates for S, both of these features can be deemed important. Therefore, to obtain a more reliable estimate for S, we need a model which incorporates both of these features.

The third method I will consider, is to model $R_V^{tc}(s)$ and $R_A^{tc}(s)$ by rescaling the QCD versions of these spectral functions. I fit measured values of $R_V^{qcd}(s)$

and $R_A^{qcd}(s)$ with superpositions of Breit–Wigner resonances, and rescale their masses and widths using large–N arguments. In particular, I fit the function

$$R_\rho^{qcd}(s) = \frac{1}{4}\left(1 - \frac{4m_\pi^2}{s}\right)^{3/2} \theta(s - 4m_\pi^2) \left[\frac{m_\rho^4}{(s - m_\rho^2)^2 + m_\rho^2 \gamma_\rho(s)^2}\right], \tag{4.17}$$

where

$$\gamma_\rho(s) = \frac{g_{\rho\pi\pi}^2}{48\pi}\frac{s}{m_\rho}\left(1 - \frac{4m_\pi^2}{s}\right)^{3/2} \theta(s - 4m_\pi^2), \tag{4.18}$$

to the QCD ρ–resonance, and rescale to

$$R_\rho^{tc}(s) = \frac{1}{4}\left[1 + \sum_i \left(1 - \frac{4M_{P_i}^2}{s}\right)^{3/2} \theta(s - 4M_{P_i}^2)\right] \left[\frac{M_\rho^4}{(s - M_\rho^2)^2 + M_\rho^2 \Gamma_\rho(s)^2}\right], \tag{4.19}$$

where

$$\Gamma_\rho(s) = \frac{G_{\rho\pi\pi}^2}{48\pi}\frac{s}{M_\rho}\left[1 + \sum_i \left(1 - \frac{4M_{P_i}^2}{s}\right)^{3/2} \theta(s - 4M_{P_i}^2)\right], \tag{4.20}$$

to obtain the techni–ρ contribution to $R_V^{tc}(s)$. Note that Eq. (4.19) has the desired property of smoothly connecting the chiral perturbation formula Eq. (4.15) onto the Breit–Wigner resonance of the techni–ρ.

Since further details of this procedure have been presented elsewhere,[3] I will simply quote the results. For the minimal technicolor case with $N_{tf} = 2$, the spectral functions obtained from rescaling are shown in figure 4, for the three cases $N_{tc} = 2$, 3, and 4. Plugging these functions into Eq. (4.8) and integrating numerically, we find

$$\begin{aligned} S &\approx 0.22 \qquad N_{tc} = 2, \\ &\approx 0.32 \qquad N_{tc} = 3, \\ &\approx 0.45 \qquad N_{tc} = 4, \end{aligned} \tag{4.21}$$

for the reference Higgs boson mass $m_H = 1\text{TeV}$. The value of S given here for the $N_{tc} = 3$ case should be fairly accurate since the technicolor spectral functions for this case can be expected to be exact scaled up replicas of their QCD counterparts. I estimate an error of ± 0.03 for this case due to uncertainties in the original QCD spectral functions. For the $N_{tc} = 2$ and $N_{tc} = 4$ cases, large–N rescaling will introduce additional uncertainties which are probably around $20 \sim 30\%$.

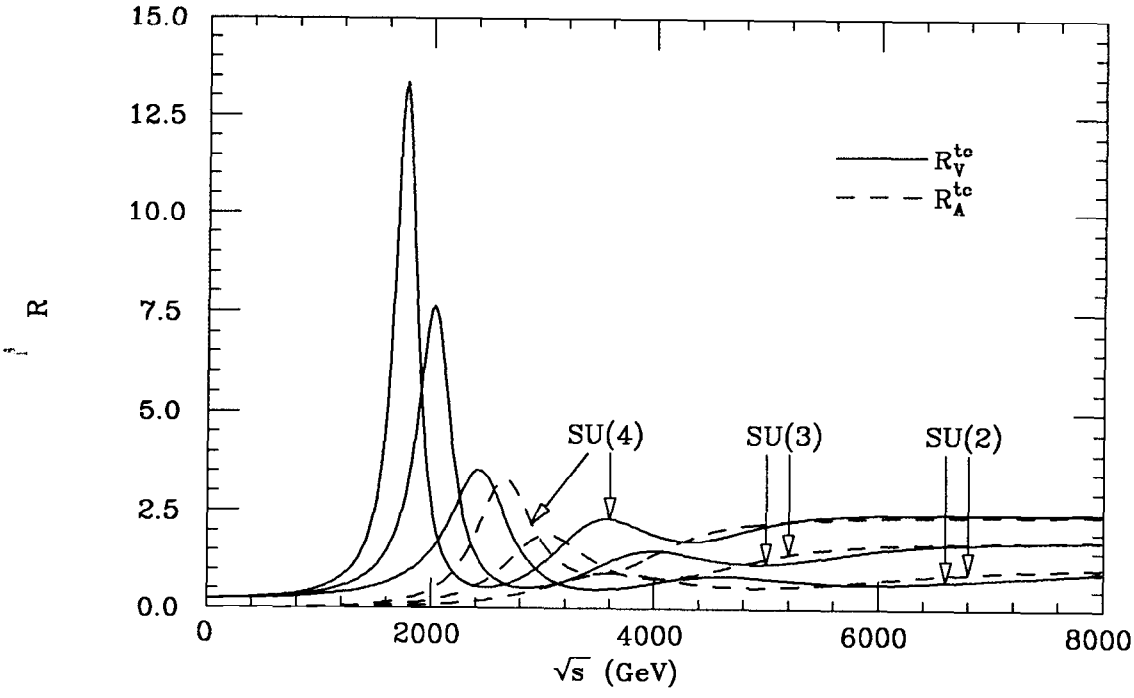

Figure 4. The spectral functions for minimal technicolor ($N_{tf} = 2$).

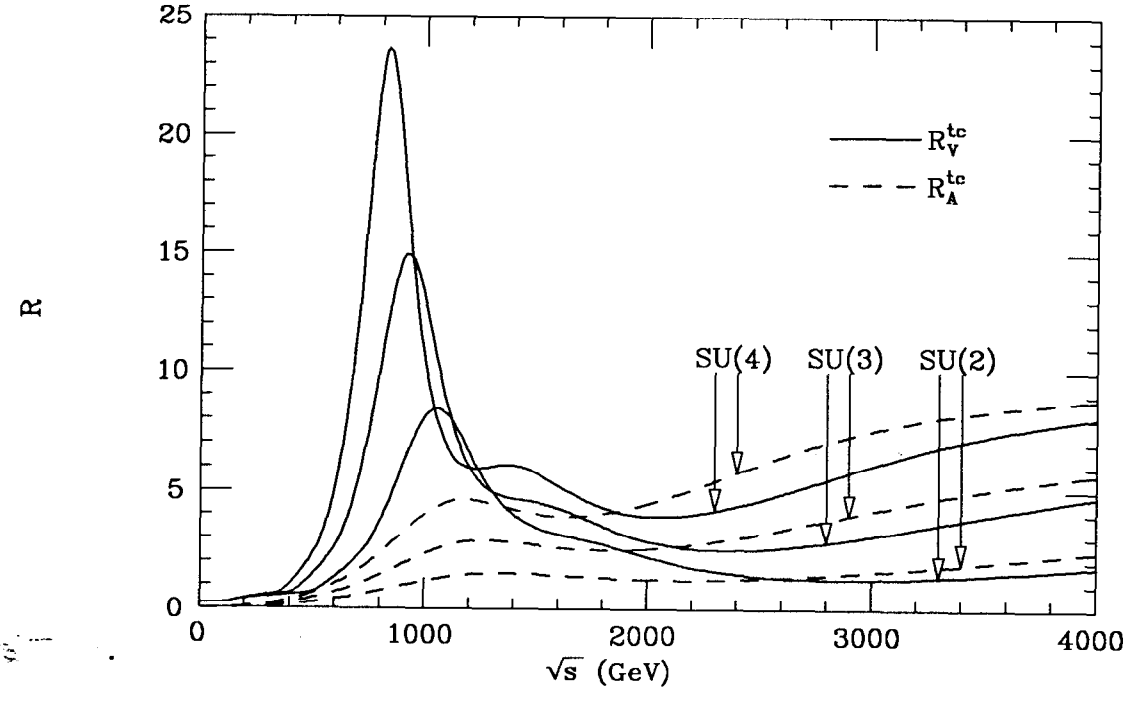

Figure 5. The spectral functions for one-generation technicolor ($N_{tf} = 8$).

For the one–generation technicolor case with $N_{tf} = 2$, the spectral functions obtained from rescaling are shown in figure 5, again for the three cases $N_{tc} = 2$, 3, and 4. The values of the PGB masses used in Eq. (4.19) were taken from ref. 19. Numerical integration gives us

$$\begin{aligned} S &\approx 0.80 \qquad N_{tc} = 2, \\ &\approx 1.20 \qquad N_{tc} = 3, \\ &\approx 1.62 \qquad N_{tc} = 4, \end{aligned} \tag{4.22}$$

for $m_H = 1\text{TeV}$. These values should again be assigned $20 \sim 30\%$ errors from large–N rescaling.

An interesting point about the estimates given in Eqs. (4.21) and (4.22) is that they can be described fairly accurately with the simple formula

$$S \approx 0.3 \frac{N_{tc}}{3} \frac{N_{tf}}{2}, \tag{4.23}$$

which is slightly larger than the vector meson dominance result Eq. (4.14), but with the same dependence on N_{tc} and N_{tf}. There is no evidence of the N_{tf}^2 dependence coming from PGB contributions, though they are included in our model.

5. Walking Technicolor

Technicolor theories with QCD–like dynamics are known to be plagued by FCNC's when ETC interactions are introduced to give masses to the quarks and leptons. A class of technicolor theories called 'walking' technicolor[20,21], whose dynamics is assumed to be quite different from that of QCD, are believed to alleviate this problem.

Let us consider how walking dynamics may modify the behavior of the spectral functions $R_V^{tc}(s)$ and $R_A^{tc}(s)$. In walking technicolor theories, the technicolor coupling $\alpha_{tc}(q^2)$ is assumed to run slowly, *i.e.* 'walk', so that it stays close to the critical coupling for chiral symmetry breaking α_c for a large momentum range before achieving asymptotic freedom as $q^2 \to \infty$. One immediate consequence of this assumption is that $R_V^{tc}(s)$ and $R_A^{tc}(s)$ will not reach their asymptotic free–technifermion values until a higher momentum compared to the usual running case. Therefore, we can expect to see more structure in these spectral functions before they become flat.

Another way to see this is to consider how the Weinberg sum rules could be modified by walking. Sundrum and Hsu[22] show that for walking technicolor theories, the left hand side of Eq. (4.9) falls like $1/q^2$ instead of $1/q^4$ in the momentum region where $\alpha_{tc}(q^2) \sim \alpha_c$. If we consider the limit in which this subasymptotic behavior persists all the way up to $q^2 \to \infty$, the Weinberg sum rules will be modified to

$$\begin{aligned} \int_0^\infty ds \left[R_V^{tc}(s) - R_A^{tc}(s)\right] &= 12\pi^2 F_\pi^2, \\ \int_0^\infty ds\, s \left[R_V^{tc}(s) - R_A^{tc}(s)\right] &= 12\pi^2 \Lambda^4 \frac{N_{tc}}{3}\frac{N_{tf}}{2}, \end{aligned} \tag{5.1}$$

where Λ is of the order of the technicolor scale. Since the first Weinberg sum rule is unmodified, the total spectral weight under $R_V^{tc}(s) - R_A^{tc}(s)$ is the same as the running case. However, change in the right hand side of the second Weinberg sum rule shows that walking will shift this spectral weight to higher momenta.

The problem is how this shift of spectral weight will affect the value of S. Let us use the vector meson dominance model to estimate this effect. If we plug the expressions Eq. (4.11) into Eq. (5.1), we find that Eq. (4.12) will be modified to

$$\begin{aligned} F_\rho^2 &= \frac{M_{a_1}^2 F_\pi^2}{M_{a_1}^2 - M_\rho^2} - \frac{\Lambda^4}{M_{a_1}^2 - M_\rho^2}\frac{N_{tc}}{3}\frac{N_{tf}}{2}, \\ F_{a_1}^2 &= \frac{M_\rho^2 F_\pi^2}{M_{a_1}^2 - M_\rho^2} - \frac{\Lambda^4}{M_{a_1}^2 - M_\rho^2}\frac{N_{tc}}{3}\frac{N_{tf}}{2}. \end{aligned} \tag{5.2}$$

This changes the estimate of S by

$$\Delta S = -\frac{4\pi\Lambda^4}{M_{a_1}^2 M_\rho^2}\frac{N_{tc}}{3}\frac{N_{tf}}{2} \approx -\frac{4\pi\lambda^4}{m_{a_1}^2 m_\rho^2}\frac{N_{tc}}{3}\frac{N_{tf}}{2}, \tag{5.3}$$

where I have assumed that large–N rescaling from QCD is still valid. Sundrum and Hsu estimate the value of λ to be $\lambda = 300\text{MeV}$.[22] Using this value, we find

$$\Delta S \approx -0.11\frac{N_{tc}}{3}\frac{N_{tf}}{2}. \tag{5.4}$$

This is a significant decrease in the value of S. However, it should be noted that this model assumes that the shift of spectral weight occurs only between the

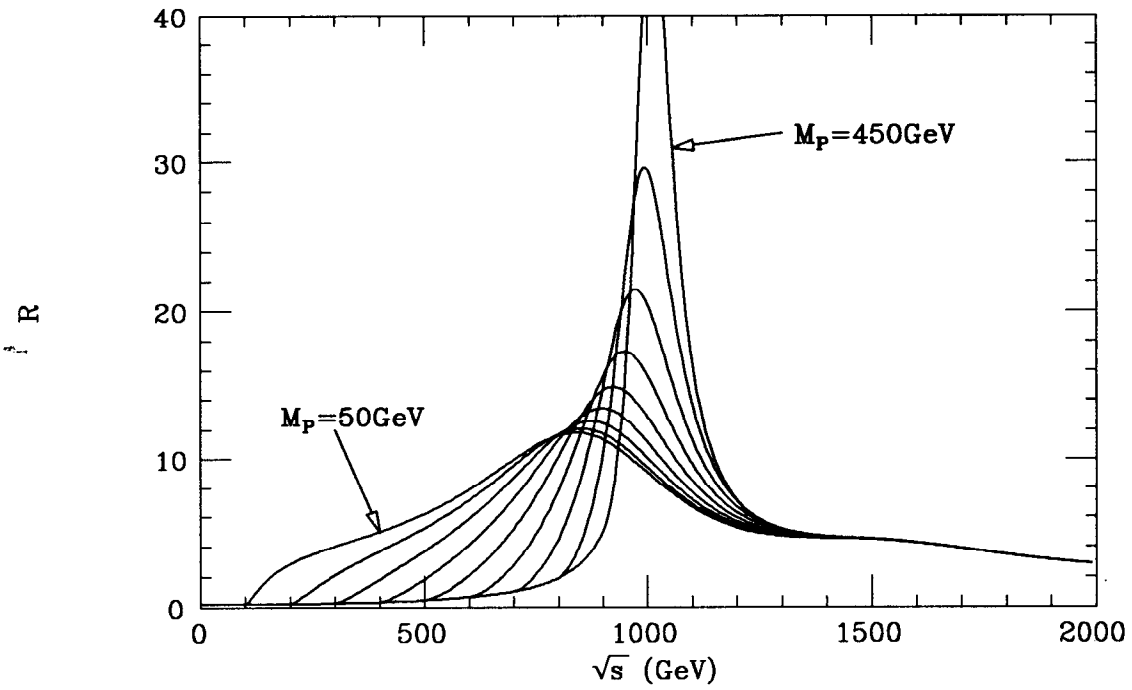

Figure 6. The shape of the techni–ρ resonance for various values of the PGB mass M_P. M_P is varied from 50GeV to 450GeV at 50GeV intervals.

lowest lying resonances. If the shift of spectral weight occurs at higher momenta also, the decrease in S will be smaller. Also, the modified second Weinberg sum rule given in Eq. (5.1) only applies in the non–walking limit in which $\alpha_{tc}(q^2)$ has a non–zero ultraviolet fixed point. For less extreme cases where asymptotic freedom is maintained, the original second Weinberg sum rule is still valid. This means that the actual shift of spectral weight in walking technicolor will be less drastic than implied by Eq. (5.1).

Another important effect of walking is that the ETC induced masses of the PGB's will be larger due to the enhancement of the technifermion condensate.[20,21] Eq. (4.16) suggest that this effect could also lead to a significant decrease of S. For instance, if all the PGB masses are doubled in Eq. (4.16), the estimate for S will change by

$$\Delta S \approx -\frac{\log 2}{6\pi}\left(\frac{N_{tf}^2}{4}-1\right). \tag{5.5}$$

For the $N_{tf}=8$ case this gives $\Delta S = -0.55$. However, increasing the PGB masses also has the effect of making the techni–ρ a narrower and more prominent resonance. This effect is correctly modeled by Eq. (4.19). Let me take the

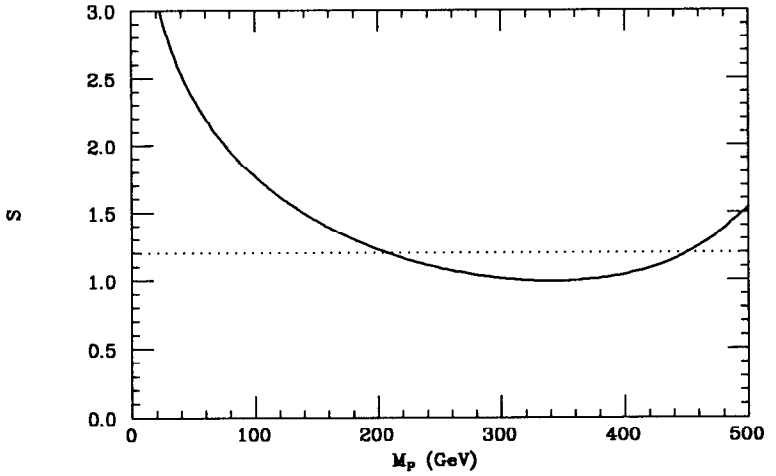

Figure 7. The M_P dependence of S in the $N_{tf} = 8$, $N_{tc} = 3$ case. The dotted line is the value of S given in Eq. (4.22).

$N_{tf} = 8$, $N_{tc} = 3$ case as an example. I give the a common mass M_P to the 15 pairs of PGB's in this model, and plot the function $R_\rho^{tc}(s)$ for $M_P = 50$GeV up to 450GeV at 50GeV intervals in figure 6. When the PGB's are light (heavy), we can see that the techni–ρ is very broad (narrow). If I calculate S numerically for various values of M_P while keeping the other parts of $R_V^{tc}(s)$ and $R_A^{tc}(s)$ fixed, I find the result shown in figure 7. For small M_P, the value of S is vary large. As M_P increases, S decreases at first. But when M_P increases beyond a certain point, the prominence of the techni–ρ will contribute to increase S instead. The minimum value of $S \approx 1.0$ is obtained for $M_P \approx 340$GeV which is only a decrease of 0.2 compared to Eq. (4.22).

Therefore, while walking will definitely lead to smaller values of S compared to the running case, the decrease in S will not be as large as Eqs. (5.4) and (5.5) may suggest. Since I assign a $20 \sim 30\%$ error to the estimate Eq. (4.23) anyway, such a decrease can be lost in this noise of large–N rescaling.

6. Comparison with Experimental Limits

In section 4, I obtained an estimate for S in technicolor theories given by Eq. (4.23). In section 5, I claimed that walking will not decrease this estimate significantly. Let us now compare these results with the experimental limits on S and T from section 3.

If I assume a uniform prior probability to all values of S and T, the limits given in Eq. (3.3) correspond to the following upper limits on S.

$$\begin{aligned} S &< -0.13 \qquad (90\%), \\ S &< \ \ 0.14 \qquad (95\%). \end{aligned} \tag{6.1}$$

These values are shown with notches on the lower part of figure 3. Comparing with Eq. (4.23), I find that the 95% upper limit on S corresponds to

$$N_{tc}N_{tf} \lesssim 3 \qquad (95\%), \tag{6.2}$$

which seems to rule out all possible values of N_{tc} and N_{tf}. However, the limits given in Eq. (6.1) are based on the assumption that, a priori, all values of S and T are equally likely. If I am prejudiced that certain values of S are a priori more likely than others, the limits will be different. In particular, if I believe that technicolor is correct, I would assume a priori that S is positive. In this case, the posterior probability distribution of S would be a Gaussian truncated below $S = 0$, and the upper limits on S will be

$$\begin{aligned} S &< 0.72 \qquad (90\%), \\ S &< 0.90 \qquad (95\%). \end{aligned} \tag{6.3}$$

This corresponds to

$$N_{tc}N_{tf} \lesssim 18 \qquad (95\%). \tag{6.4}$$

For the one generation case with $N_{tf} = 8$, this rules out $N_{tc} \gtrsim 3$.

For walking technicolor, the limit on $N_{tc}N_{tf}$ will be slightly weaker. However, walking technicolor models usually require a large number of technifermion doublets to slow down the running of the coupling. It would be very difficult to keep N_{tf} within the experimentally allowed region and achieve walking at the same time.

I emphasize here that these limits on $N_{tc}N_{tf}$ are placed on technicolor theories without any isospin or parity violation. Since such theories are unrealistic to begin with, it is no big loss that a large portion of them have been ruled out. More realistic theories will necessarily entail large isospin splittings, especially if they are to reproduce the observed t–b mass difference.

For technicolor theories with isospin splitting, estimating S and T would be more difficult since such splittings come from ETC interactions whose effects are difficult to decipher. However, the extra isospin violating contribution to S can potentially make S negative and compatible with the experimental limits. A more difficult problem in this case is the experimental limit placed on T, since isospin breaking effects tend to contribute to make T positive and large. But eventually, the question will always come back to whether we can estimate S and T reliably in this case at all. This remains an open problem to be pursued in the future.

Acknowledgements

I am grateful to M. E. Peskin, from whom I learned a great deal through our collaboration on this project, and to J. Bjorken, M. Golden, S. Hsu, D. Kennedy, K. Lane, P. Langacker, B. Lynn, L. Randall, J. Rosner, R. Sundrum, K. Takeuchi, and T. Truong for helpful discussions. I would also like to thank M. N. Rebelo and A. Falk for their critical reading of this manuscript.

Appendix

The following numbers are evaluated with $m_t = 150\text{GeV}$, $m_H = 1\text{TeV}$, $e^2 = 4\pi\alpha_{*,0}(m_Z^2) = 4\pi/129$, $s^2 = 0.23$, and $\alpha_s = 0.12$. The constant terms on the right hand sides are the Standard Model predictions including both oblique and direct corrections, and the QCD corrections.

$$
\begin{aligned}
g_L^2 &= 0.3001 - [2.67\times10^{-3}]S + [6.53\times10^{-3}]T \\
g_R^2 &= 0.0302 + [9.17\times10^{-4}]S - [1.94\times10^{-4}]T \\
m_W/m_Z &= 0.8787 - [3.15\times10^{-3}]S + [4.86\times10^{-3}]T + [3.70\times10^{-3}]U \\
\Gamma_Z &= 2.484 - [9.58\times10^{-3}]S + [2.615\times10^{-2}]T \quad (\text{GeV}) \\
R_Z = \Gamma_{\text{had}}/\Gamma_{\ell^+\ell^-} &= 20.78 - [5.99\times10^{-2}]S + [4.24\times10^{-2}]T \\
A_{FB}^{\ell} &= 0.0126 - [6.72\times10^{-3}]S + [4.76\times10^{-3}]T \\
A_{FB}^{b} &= 0.0848 - [1.97\times10^{-2}]S + [1.40\times10^{-2}]T \\
A_{LR} = -P_\tau &= 0.1297 - [2.82\times10^{-2}]S + [2.00\times10^{-2}]T \\
Q_W({}^{133}_{55}Cs) &= -73.31 - 0.790S - 0.011T
\end{aligned}
$$

References

1. J. F. Gunion, H. E. Haber, G. Kane, and S. Dawson, *The Higgs Hunter's Guide*, section 2.5 (Addison–Wesley, Redwood City, 1990).
2. D. C. Kennedy and B. W. Lynn, *Nucl. Phys.* **B322** (1989) 1; B. W. Lynn, SLAC-PUB-5077 (1989); M. Kuroda, G. Moultaka, and D. Schildknecht, *Nucl. Phys.* **B350** (1991) 25; D..C. Kennedy, 1991 TASI Lectures.
3. M. E. Peskin and T. Takeuchi, SLAC Report No. SLAC-PUB-5618, to be published in *Phys. Rev.* **D** .
4. T. Takeuchi, SLAC Report No. SLAC-PUB-5619, to be published in *the Proceedings of the 1991 Nagoya Spring School on Dynamical Symmetry Breaking* (World Scientific, Singapore).
5. P. Langacker, in *the Review of Particle Properties*, page III.56, *Phys. Lett.* **B239** (1990) 1.
6. The CDF Collaboration, F. Abe *et al.*, *Phys. Rev. Lett.* **65** (1990) 2243; *Phys. Rev.* **D43** (1991) 2070; The UA2 Collaboration, J. Alitti *et al.*, CERN Report No. CERN-PPE/91-163 (1991).
7. The LEP Collaborations: ALEPH, DELPHI, L3, and OPAL, CERN Report No. CERN-PPE/91-232 (1991).

8. J. R. Carter, talk presented at the 1991 Joint International Lepton–Photon Symposium and Europhysics Conference on High Energy Physics, Jul. 25 – Aug. 1, 1991.

9. M. C. Noecker, B. P. Masterson, and C. E. Wieman, *Phys. Rev. Lett.* **61** (1988) 310; S. A. Blundell, W. R. Johnson, and J. Sapirstein, *Phys. Rev. Lett.* **65** (1990) 1411.

10. M. E. Peskin and T. Takeuchi, *Phys. Rev. Lett.* **65** (1990) 964.

11. W. J. Marciano and J. L. Rosner, *Phys. Rev. Lett.* **65** (1990) 2963.

12. D. C. Kennedy and P. Langacker, *Phys. Rev. Lett.* **65** (1990) 2967, E: **66** (1991) 395; *Phys. Rev.* **D44** (1991) 1591.

13. G. Altarelli and R. Barbieri, *Phys. Lett.* **B253** (1991) 161; G. Altarelli, R. Barbieri, and S. Jadach, CERN Report No. CERN-TH-6124-91.

14. A. Ali and G. Degrassi, DESY Report No. DESY-91-035, to be published in the *M. A. B. Bég Memorial Volume* (World Scientific, Singapore).

15. G. Bhattacharyya, S. Banerjee, and P. Roy, Tata Institute Report No. TIFR-TH-91-38.

16. P. Renton, Oxford University Report No. OUNP-91-30.

17. C. Bernard, A. Duncan, J. LoSecco, and S. Weinberg, *Phys. Rev.* **D12** (1975) 792.

18. S. Weinberg, *Phys. Rev. Lett.* **18** (1967) 507.

19. M. E. Peskin, *Nucl. Phys.* **B175** (1980) 197;
J. P. Preskill, *Nucl. Phys.* **B177** (1981) 21.

20. B. Holdom, *Phys. Rev.* **D24** (1981) 1441; *Phys. Lett.* **B198** (1987) 535.

21. T. Appelquist and L. C. R. Wijewardhana, *Phys. Rev.* **D35** (1987) 774; *Phys. Rev.* **D36** (1987) 568.

22. R. Sundrum and S. D. H. Hsu, LBL Report No. LBL-31066 (1991).